Published in final edited form as:
Exp Cell Res. 2009 August 15; 315(14): 2420–2432. doi:10.1016/j.yexcr.2009.05.004.

Evidence for a direct involvement of hMSH5 in promoting ionizing radiation induced apoptosis

JOSHUA D. TOMPKINS, **XILING WU**, **YEN-LIN CHU**, and **CHENGTAO HER***
School of Molecular Biosciences and Center for Reproductive Biology, PO Box 644660, Washington State University, Pullman, WA 99164-4660

Abstract

Although increasing evidence has suggested that the hMSH5 protein plays an important role in meiotic and mitotic DNA recombinational repair, its precise functions in recombination and DNA damage response are presently elusive. Here we show that the interaction between hMSH5 and c-Abl confers ionizing radiation (IR)-induced apoptotic response by promoting c-Abl activation and p73 accumulation, and these effects are greatly enhanced in cells expressing $hMSH5^{P29S}$ (i.e. the hMSH5 variant possessing a proline to serine change within the N-terminal $(Px)_5$ dipep-tide repeat). Our current study provides the first evidence that the $(Px)_5$ dipeptide repeat plays an important role in modulating the interaction between hMSH5 and c-Abl and alteration of this dipeptide repeat in $hMSH5^{P29S}$ leads to increased IR sensitivity owing to enhanced caspase-3-mediated apoptosis. In addition, RNAi-mediated hMSH5 silencing leads to the reduction of apoptosis in IR-treated cells. In short, this study implicates a role for hMSH5 in DNA damage response involving c-Abl and p73, and suggests that mutations impairing this process could significantly affect normal cellular responses to anti-cancer treatments.

Keywords

hMSH5; $hMSH5^{P29S}$; c-Abl; apoptosis; p73; ionizing radiation; DNA damage response

INTRODUCTION

The human MutS homolog hMSH5 is a member of the mismatch repair (MMR) family of proteins [1]. However at present there is no evidence to suggest its involvement in MMR, but instead recent studies have suggested potential roles for hMSH5 in DNA double strand break (DSB) repair during meiosis as well as in the process of mitotic recombination [2–5]. Purified hMSH4-hMSH5 protein complexes have been shown to possess binding activities for DSB repair intermediate structures including the Holliday junction (HJ) [6]. The human hMSH5 has also been implicated in the process of class switch recombination during B and T cell development [4], however similar studies performed with two different *Msh5* mutant mouse lines have produced conflicting results [4,7]. It is interesting to note that these two mouse lines have also been reported to display different degrees of meiotic chromosome pairing defects [2,3], suggesting the role of *Msh5* might be influenced by potential difference in their genetic backgrounds. The human hMSH5 has also been shown to interact

*Address all correspondence and reprint requests to: Dr. Chengtao Her at above address. Telephone: (509) 335-7537, Fax#: (509) 335-4159, cher@wsu.edu.

with a newly identified HJ binding protein and with hMRE11 in human alveolar basal epithelial cell derived lung adenocarcinoma A549 cells [5]. In addition, the *hMSH5* locus at 6p21.33 has been identified as one of the risk loci for lung cancer in a genome-wide association study [8]. These observations have highlighted a need for a better understanding of the functions of this protein in humans.

We have previously reported that the human hMSH5 protein interacts with c-Abl [9]. It is known that the c-Abl tyrosine kinase can be activated by the sensor kinase ataxia telangiectasia mutated (ATM) in response to IR-induced DNA damage [10,11]. The phenotypic outcomes (i.e., DNA repair, cell cycle arrest, and apoptosis) are tailored by the dynamic interplay between activated c-Abl and an array of downstream protein factors that are involved in DNA repair and the initiation of apoptosis (for review see [12]). Given the well-established role of c-Abl in the regulation of recombinational repair and DNA damage response [12–14], it is plausible that, in addition to recombinational repair, the hMSH5-c-Abl interaction may also play a role in the regulation of DNA damage response. In fact, there are numerous instances where DNA repair proteins can exert damage signaling properties [15].

The activity of c-Abl tyrosine kinase is regulated by the concerted actions of intra-molecular scaffolds, cellular regulators, and autophosphorylation—which collectively modulate its multifaceted actions in cell proliferation, DNA damage response, and apoptosis (for reviews see [16,17]). Among various functions, the c-Abl dependent apoptotic response often involves the activation of the downstream factor p73; as such the stabilized and phosphorylated p73 can further activate pro-apoptotic factors [18–20]. Although DNA damage-induced c-Abl activation can trigger apoptosis, constitutively active c-Abl fusions (e.g. Bcr-Abl) are, however, often oncogenic and anti-apoptotic through nuclear exclusion during the development of chronic myeloid and acute lymphoblastic leukemias [21]. Furthermore, steady activation of c-Abl at a moderate level is involved in the development of lung and breast tumors [22]. Therefore, it is likely that the role of c-Abl in promoting either apoptosis or proliferation is fine-tuned by the extent of cAbl activation, in particular during the processes of DNA damage response and carcinogenesis.

In the current study, we have investigated the functional roles of the hMSH5-c-Abl interaction in mediating cellular responses to IR-induced DNA damage with a special emphasis on the effects elicited by the common hMSH5 variant ($hMSH5^{P29S}$) that displays an altered interaction with c-Abl. Our study demonstrates, for the first time, that the human hMSH5 protein regulates c-Abl in cellular response to IR-induced DNA damage.

MATERIALS AND METHODS

Yeast two-hybrid analysis

β-galactosidase liquid assays were performed in L40 yeast as previously described [23]. Briefly, DNA fragments that encode $hMSH5^{1–109}$ and the corresponding deletion mutants as well as the mouse $Msh5^{1–108}$ were generated by PCR and cloned into pGADT7 vector (Clontech, Palo Alto, CA). Nucleotide mutations were generated by PCR-based site-directed mutagenesis and verified by restriction digest and DNA sequencing analyses. The pBTMd/c-Abl SH3 construct was created previously [9]. To determine the relative protein interaction strength, L40 double transformants expressing corresponding fusion proteins were used to monitor the levels of transcription activation of the *lacZ* reporter gene. Fusion protein expression in L40 was validated by immunoblotting analysis. All interactions were assessed from at least three independent experiments.

Cell culture and preparation of cell extract

All cell lines were maintained in DMEM (Invitrogen, Carlsbad, CA) containing 10% FBS (Gib-co-Invitrogen) and 1% Penicillin-Streptomycin (Invitrogen). Whole cell extracts were prepared with the T-PER Tissue Protein Extraction Reagent (Pierce, Rockford, IL) supplemented with 1x complete EDTA-free protease inhibitor cocktail (Roche, Indianapolis, IN). Briefly, cells pelleted from 10-cm dishes were washed with 1x PBS and lysed with approximately 300 μL of T-PER on ice for 20 min with intermittent vortexing followed by centrifugation at 14,000 × g at 4°C to isolate soluble extracts. For endogenous hMSH5 detection, protein extracts were routinely prepared from cell pellets obtained from 15-cm dishes with an extended duration (~ 40 min) of incubation on ice in 150 – 300 μL of T-PER. HeLa and 293T cell pellets were also alternatively obtained from the National Cell Culture Center (Minneapolis, MN) with cell extracts prepared in CelLyt-ic-M cell Lysis Reagent (Sigma, St. Louis, MO).

Co-immunoprecipitation and Western blotting

Ten μg of relevant antibodies were used to perform co-IP analysis. Immunoprecipitates were captured with 40 μl of 50% slurry of BSA-saturated Protein A/rProtein G-Agarose (Invitrogen). Immunoprecipitated proteins or cell extracts were separated by 7.5–20% SDS-PAGE and were transferred to nitrocellulose membranes (Bio-Rad Laboratories, Hercules, CA) for immunoblotting analysis performed with the ECL Western blotting system (Amersham Biosciences, Little Chalfont Buchinghamshire, UK). Antibodies used in the present study include the following: α-myc (Clontech), 1:500; α-hMSH4 [24], 1:2000; α-hMSH5 [25], 1:1500; α-FLAG M2 (Sigma), 1:1000; α- α-tubulin (DM1A; Sigma), 1:1000; α-c-Abl (8E9; BD PharMingen, San Diego, CA), 1:400; α-phospho-(Tyr^{245})-c-Abl (Cell Signaling, Beverly, MA), 1:750; α-pTyr (P-Tyr-100, Cell Signaling), 1:1000; α-p73 (GC-15; Calbiochem, EMD, San Diego, CA), 1:200; α-active cas-pase-3 (rabbit polyclonal, Millipore, Temecula, CA), 1:200; α-GAL4 AD (Clontech), 1:250; α-LexA (D-19, Santa Cruz Biotechnology, Santa Cruz, CA), 1:100. Additionally, a mouse antibody against hMSH5 was also generated with recombinant hMSH5 cp-1 protein as an antigen [25] (Invitrogen/Zymed Laboratories, San Francisco, CA), 1:1500. Secondary antibodies used in this study included GAM-HRP, GAR-HRP, and DAG-HRP (Bio-Rad Laboratories), 1:2000.

Stable and transient transfections of 293T cells

The generation of the stable 293T/hMSH5^{P29S} cell line was accomplished by a previously described procedure that was successfully used to generate the 293T/hMSH5 cell line [25]. Briefly, 293T cells were transfected with pcDNA6(Bsd)/flag-hMSH5^{P29S} expression vector, and transfected cells were selected with 10 μg/ml blasticidin (Invitrogen) to create stable clones. Transient transfection of 293T, 293T/hMSH5, and 293T/hMSH5^{P29S} cell lines was carried out by the use of a standard calcium-phosphate procedure [9]. The mammalian expression construct pcDNA3.1-myc/c-Abl was generated previously [9]. To analyze the effects of co-expression of c-Abl with full-length hMSH5 or hMSH5ΔN, 293T cells were co-transfected to express c-Abl together with various forms of hMSH5. The hMSH5 RNAi-directed hMSH5 knockdown was performed with an shRNA encoding construct, pmH1P-Bsd/hMSH5 sh-2, targeting hMSH5 ORF at nucleotide positions 1031–1049 (5′-TGGGCCTGAGGGATGCCTG), and the RNAi-mediated c-Abl knockdown was achieved by transfection of cells with pmHIP-Neo/c-Abl sh-2, targeting cAbl ORF at nucleotide positions 613–631 (5′-GTGGCCGACGGGCTCATCA). Efficiency of RNAi-mediated knockdown was determined by immunoblotting analyses of cell extracts at 48 h after transfection. Empty pmH1P-Neo vector or pmH1P-Neo/NT (NT: non-targeting) was used for RNAi specificity controls. The expression construct pcDNA6(Bsd)/flag-hMSH5$^{116–834}$ was derived from pcDNA6(Bsd)/flag-hMSH5 by deleting a Hind III fragment that encodes

the first 115 amino acids of hMSH5—the resulting N-terminal-truncated flag-tagged hMSH5 is hereafter referred to as hMSH5ΔN.

Imatinib and IR treatment

Inhibition of c-Abl kinase in cultured cells was commenced 48 h prior to planned experiments with 4 μM of imatinib (previously STI-571) (Novartis, Basel, Switzerland), and the inhibition of c-Abl kinase remained to be enforced when the duration of cell culture was additionally extended. Irradiation of cells with IR was conducted at room temperature with a cobalt-60 source (Nuclear Radiation Center, Washington State University) with a dose rate of 11 Gy/min or 6.6 Gy/min.

TUNEL assay

Apoptosis was analyzed by the use of a fluorescein-based *In Situ* Cell Death Detection Kit (Roche) according to the manufacturer's recommendations. Briefly, 293T, 293T/hMSH5, and 293T/hMSH5^{P29S} cells were treated with 2, 5, and 10 Gy IR and maintained in culture for an additional 24 h before TUNEL analysis. To analyze the effects of hMSH5 RNAi on apoptosis, 293T cells were transfected with the pmH1P-Bsd/hMSH5 sh-2 vector at 48 h prior to irradiation with 5 Gy IR. Transfected 293T cells (expressing hMSH5, hMSH5^{P29S}, and hMSH5ΔN) were irradiated with 5 Gy IR at 48 h post transfection, and TUNEL assay was performed at 24 h after IR treatment, for which the untreated mock transfected cells were used as negative controls. Cells that displayed positive TUNEL and DAPI staining were analyzed by fluorescent microscopy with cell numbers recorded from multiple locations on the slides. Approximately 200 cells were examined from each of at least three different view fields (total cell counts > 600).

Clonogenic cell survival assay

To perform clonogenic survival assay, triplicate 10-cm plates containing 293T, 293T/hMSH5, and 293T/hMSH5^{P29S} cells, seeded at a density of 5000 cells per plate, were exposed to 1, 2, and 3 Gy IR. Irradiated cells were maintained in culture for approximately 10 days to allow colony formation. Colonies were visualized with Crystal Violet (Sigma) and those containing at least 50 cells were recorded. The percentage of cell survival was then determined in reference to untreated controls for each cell line. Data represents the mean of three individual experiments and error bars represent standard deviations of the mean.

RESULTS

The $(Px)_5$ motif of hMSH5 modulates its interaction with c-Abl

It has been demonstrated previously that the interaction between hMSH5 and c-Abl is mediated by the c-Abl SH3 domain and the NH_2-terminal proline-rich region of hMSH5 (i.e. aa 1–109), of which the latter contains a $(Px)_5$ dipeptide repeat flanked by two PxxP motifs [9]. Interestingly, the disruption of the $(Px)_5$ dipeptide repeat in the hMSH5P29S variant, encoded by a common polymorphic allele *hMSH5*^{C85T}, has been potentially linked to the occurrence of ovarian cancer and premature ovarian failure [25,26]. To investigate the role of the $(Px)_5$ dipeptide repeat in c-Abl interaction, we performed β-galactosidase based yeast two-hybrid liquid assays to determine the relative interaction strength between c-Abl SH3 domain and a series of hMSH5 deletions as depicted in Fig. 1A. Immunoblotting analysis confirmed the expression of all relevant proteins in yeast reporter strain L40 (data not shown).

Interestingly, the Pro to Ser change at the center of the $(Px)_5$ motif has enhanced the physical interaction between the two proteins, however deletion of all five Pro residues of

the $(Px)_5$ motif (i.e. pdel) has reduced the interaction by approximately 60%, and further deletion of the first PxxP motif (i.e. ΔNpdel) caused an additional 15% reduction of the interaction (Fig. 1B). Moreover, the c-Abl interacting domain on hMSH5 appears to be highly conserved as the comparable portion of the mouse Msh5 interacted strongly with c-Abl (Fig. 1B), for which the increased interaction strength could be explained by the presence of the third PxxP motif in the mouse Msh5 located in a region corresponding to the human $(Px)_5$ motif (Fig. 1A, arrows). It is of interest to note that the locations of the two PxxP motifs are conserved, but not the sequence surrounding the first PxxP motif (Fig. 1A). Together, these observations indicate that the interaction between hMSH5 and the c-Abl SH3 domain is mediated by both the $(Px)_5$ dipeptide repeat and the PxxP motifs, of which the $(Px)_5$ repeat modulates the interaction between these two proteins.

Endogenous hMSH5 physically interacts with c-Abl and undergoes c-Abl dependent tyrosine phosphorylated in response to IR

In order to establish a foundation to explore the biological effects of $hMSH5^{P29S}$ in mitotic cells, we have first performed co-immunoprecipitation (co-IP) experiments to validate the interaction between endogenous hMSH5 and c-Abl in two human cell lines. Co-IP was performed with a newly generated mouse α-hMSH5 antiserum. Similar to that of the affinity-purified rabbit α-hMSH5 antibody [25], the new antiserum specifically recognized both hMSH5 cp-1 (i.e., the antigen) expressed in BL21 cells and the exogenously expressed full-length hMSH5 in 293T cells (Fig. 2A). Co-IP analysis of HeLa and 293T cell extracts has clearly demonstrated that the endogenous hMSH5 interacts with c-Abl (Fig. 2B). It should be noted that expression levels of hMSH5 in these two cell lines are relatively low, so detection of endogenous hMSH5 usually requires either a large amount of cell extract or IP prior to immunoblotting. To test whether IR-triggered tyrosine phosphorylation of endogenous hMSH5 was c-Abl dependent, c-Abl kinase inhibitor imatinib and RNAi-mediated c-Abl knockdown were employed. Experiments performed with 293T cells indicated that the IR-induced hMSH5 tyrosine phosphorylation could be significantly inhibited by either imatinib treatment (Fig. 2C) or c-Abl knockdown (Fig. 2D), suggesting that the IR-induced tyrosine phosphorylation of endogenous hMSH5 is mediated by cAbl in mitotic cells.

hMSH5 promotes c-Abl autophosphorylation, IR-induced p73 accumulation, and p73 phosphorylation

The aforementioned effect of P29S on hMSH5/c-Abl interaction is highly suggestive of a potential impact of this variant on c-Abl mediated DNA damage response. Thus, we have next analyzed the effects of $hMSH5^{P29S}$ on the activation of c-Abl and p73 in stably transfected 293T cells expressing Flag-$hMSH5^{P29S}$ (designated as 293T/$hMSH5^{P29S}$) to ameliorate the lack of cell lines expressing endogenous $hMSH5^{P29S}$. The expression levels of flag-tagged hMSH5 and $hMSH5^{P29S}$ in the stable transfectants are essentially identical (Fig. 3A). Since the c-Abl auto-phosphorylation at tyrosine residue 245 (Tyr^{245}) is a prerequisite for the full activation of c-Abl tyrosine kinase [27], we first investigated whether c-Abl autophosphorylation at Tyr^{245} (Tyr^{226} in c-Abl 1a) was affected by the P29S alteration. To this end, transient expression of c-Abl was employed to compensate for the relatively high levels of hMSH5 and $hMSH5^{P29S}$ in these stable cell lines. With 293T as a basal level control, the levels of c-Abl Tyr^{245} autophosphorylation increased significantly in 293T/hMSH5 and to a greater extent in 293T/$hMSH5^{P29S}$ cells in the absence of DNA damage (Fig. 3), and this autophosphorylation could be abrogated by imatinib treatment (Fig. 3A). Immunoblotting analysis of cell extracts indicated that c-Abl Tyr^{245} auto-phosphorylation was well correlated with the level of p73 accumulation (Fig. 4A), suggesting that the level of p73 accumulation might be regulated by hMSH5-depenent c-Abl Tyr^{245} auto-phosphorylation. To this end, the association between c-Abl and p73 was

analyzed in both untreated and IR-treated 293T, 293T/hMSH5, and 293T/hMSH5^{P29S} cells. The results of these co-IP experiments indicated that the interaction between p73 and c-Abl was enhanced in 293T/hMSH5 and 293T/hMSH5^{P29S} cells, and this interaction was not affected by IR-induced p73 phosphorylation (Fig. 4B, c-Abl/p73 ratio). In comparison to that of 293T cells, the levels of IR-triggered p73 tyrosine phosphorylation were significantly higher in 293T/hMSH5 and 293T/hMSH5^{P29S} cells (Fig. 4B, bar graph). The expression levels of various proteins in parental cells were also analyzed under identical immunoblotting conditions (Fig. 4C). These observations strongly suggest that the interaction with hMSH5 enhances c-Abl autophosphorylation, which in turn strengthens the interaction between c-Abl and p73, leading to p73 accumulation and enhanced IR-triggered tyrosine phosphorylation. It is conceivable that autophosphorylation at Tyr^{245} promotes c-Abl to adapt a scaffold with improved association with p73, thereby enhancing p73 accumulation.

Enhanced c-Abl autophosphorylation and strengthened c-Abl-p73 interaction augment IR-induced caspase-3 mediated apoptotic response

It is known that the c-Abl mediated phosphorylation can induce p73 transactivation to enable pro-apoptotic factors [20,28,29]. Therefore, we next utilized TUNEL assay to analyze the levels of apoptosis in 293T, 293T/hMSH5, and 293T/hMSH5^{P29S} cells at 24 h after IR treatments. In addition, survival potentials of IR-treated 293T, 293T/hMSH5, and 293T/hMSH5^{P29S} cells were also analyzed by a 10-day clonogenic assay. The results of the TUNEL analysis indicated that hMSH5^{P29S}, or hMSH5 to a lesser extent, promoted apoptotic responses in an IR dose-dependent manner when cells were treated with 5 or 10 Gy IR (Fig. 5A). The lack of apoptosis in cells treated with 2 Gy IR is highly suggestive of a potential biphasic response that could be controlled by the interaction between hMSH5 and c-Abl (see discussion). This observation is reminiscent of an earlier study, in which the linear correlation between DSB repair and the number of γH2Ax foci was only observed in cells irradiated with IR at doses below 2 Gy [30]. In addition, the cAbl kinase inhibitor imatinib abrogated the IR-induced apoptotic response, suggesting that the IR-induced apoptosis requires c-Abl kinase activity (Fig. 5A). The results of the clonogenic survival analysis also indicated that hMSH5 or hMSH5^{P29S} expression in 293T cells led to a significant reduction of cell survival in response to IR treatment, of which hMSH5^{P29S} displayed a greater effect (Fig. 5B). Furthermore, immunoblotting analysis performed with an active cas-pase-3 antibody demonstrated that the activation of caspase-3 was an intrinsic element of the enhanced IR-induced apoptotic response in cells with elevated levels of hMSH5 or hMSH5^{P29S} (Fig. 5C), indicating that the hMSH5-c-Abl interaction mediates caspase-dependent apoptosis in response to IR-induced DNA damage.

hMSH5^{P29S} is refractory to c-Abl mediated tyrosine phosphorylation and sustains its interaction with c-Abl after IR exposure

To further investigate the molecular basis underlying the observed functional differences between hMSH5 and hMSH5^{P29S}, we assessed whether hMSH5^{P29S} could be efficiently phosphory-lated by c-Abl in response to IR-induced DNA damage, as well as the subsequent effect on the hMSH5^{P29S}-c-Abl interaction. For this purpose, 293T/hMSH5 and 293T/hMSH5^{P29S} cells were irradiated with 20 Gy IR, and the status of hMSH5 phosphorylation was analyzed by Western blotting of α-Flag immunopurified hMSH5 and hMSH5^{P29S} proteins. As shown in Fig. 6, IR-triggered c-Abl-dependent hMSH5 tyrosine phosphorylation was readily detected, however under identical conditions, hMSH5^{P29S} was refractory to tyrosine phosphorylation. This result was also recapitulated when hMSH5^{P29S} and c-Abl were co-expressed in SF9 insect cells (data not shown). Although the molecular basis underlying this observation is not known, one possible explanation is that the hMSH5^{P29S} protein can adopt a configuration that prevents phosphorylation. In addition, co-

IP analysis indicated that hMSH5 dissociated from c-Abl after tyrosine phosphorylation, whereas the hMSH5^{P29S} and c-Abl association was not disrupted by IR treatment (Fig. 6). These results demonstrate that IR-triggered hMSH5 tyrosine phosphorylation causes the dissociation of hMSH5-c-Abl complex. Therefore, hMSH5^{P29S}, through resistance to IR-triggered phosphorylation, sustains its interaction with c-Abl after IR exposure.

Together, our evidence tends to support a scenario in which the interaction with hMSH5 engages c-Abl in a pre-activation stage through autophosphorylation and the full activation of the c-Abl kinase requires additional stimuli such as IR. This view is supported by the lack of tyro-sine phosphorylation of hMSH5 and p73 prior to IR exposure and the apparent phosphorylation of these two proteins following IR treatment (Figs. 2C, 2D, 4B, and 6). Although the precise function of hMSH5 tyrosine phosphorylation is unknown, it appears that this phosphorylation may play a role in the regulation of c-Abl.

Direct c-Abl interaction is required for the involvement of hMSH5 in IR-triggered apoptosis

To test whether the hMSH5-promoted IR-induced apoptosis requires a direct interaction with cAbl, we transiently co-expressed myc-tagged c-Abl together with flag-tagged hMSH5, hMSH5^{P29S}, or hMSH5ΔN in 293T cells (Fig. 7A). The hMSH5ΔN represents a c-Abl interacting domain-deleted form of hMSH5 (see Materials and Methods for details). In contrast to hMSH5 and hMSH5^{P29S}, the expression of hMSH5ΔN did not lead to p73 accumulation by immunoblotting analysis of the transfected cells (Fig. 7A). The results of co-IP experiments indicated that hMSH5ΔN did not interact with c-Abl (Fig. 7B). In addition, 293T cells co-expressing hMSH5ΔN and c-Abl displayed lower level of c-Abl Tyr^{245} autophosphorylation in comparison to cells expressing full-length hMSH5 (Fig. 7B). Furthermore, TUNEL analysis demonstrated that hMSH5ΔN did not promote IR-induced apoptosis beyond that of the control cells, and expression of various forms of hMSH5 has no effects on apoptosis in the absence of IR exposure (Fig. 5B). These results provide additional support for the importance of the hMSH5-c-Abl interaction in IR-triggered apoptotic response.

IR-induced accumulation of endogenous hMSH5 promotes apoptosis

As the overexpression of hMSH5 can increase IR-induced apoptotic response, we next investigated whether this observation could be physiologically relevant. Thus, the endogenous levels of hMSH5, along with p73, were examined in HeLa and 293T cells following IR treatment. The results of these experiments indicated that IR promoted hMSH5 induction in both 293T and HeLa cells in a dose and time dependent manner (Figs. 8A and 8B). Significant induction of hMSH5 required at least 5 Gy IR in both HeLa and 293T cells, and 2 Gy IR could only lead to a low level of hMSH5 induction in HeLa cells (Fig. 8A).

It appeared that the accumulation of hMSH5 preceded the accumulation of p73 and reached its peak at 5 h after IR treatment in 293T cells, whereas the level of p73 gradually increased over the course of 5 to 24 h following IR exposure (Fig. 8B). The IR-induced endogenous hMSH5 accumulation was dependent on c-Abl kinase activity as imatinib treatment diminished this effect (Fig. 8C). Moreover, reduction of hMSH5 accumulation by RNAi (~ 60%) compromised IR-triggered p73 accumulation at 5 h post-IR exposure (Fig. 8C), and an approximately 50% reduction of IR-induced apoptosis at 24 h (Fig. 8D). We also noted that the RNAi-mediated knockdown of endogenous hMSH5 reduced the level of IR-triggered c-Abl phosphorylation at 5 h post-IR (Fig. 8C). As a whole, the results of these experiments are consistent with those performed with the stable cell lines overexpressing hMSH5 or hMSH5^{P29S}. Thus, this study can also serve as a springboard for future exploration of other hMSH5 nonsynonymous variants by similar strategies.

DISCUSSION

DNA damage is one of the most important factors for cancer development in humans, and yet it also contributes to the therapeutic efficacy of many anti-cancer regimens using chemo- and radiotherapeutics. Our current study suggests that the interaction between hMSH5 and c-Abl underlies a novel mechanism in mediating cellular response to IR exposure. Specifically, we demonstrate that the interaction between these two proteins plays an important role in initiating p73-mediated caspase-dependent apoptosis in response to IR-induced DNA damage. The significance of this observation is reflected by the effects of the peculiar interaction between $hMSH5^{P29S}$ and c-Abl on increasing cellular radiosensitivity.

The ability of hMSH5, or to a greater extent $hMSH5^{P29S}$, to stimulate damage-independent c-Abl autophosphorylation at Tyr^{245} could be largely attributed to the strengthened physical interaction between hMSH5 proline-rich NH_2-terminal region and c-Abl SH3 domain as indicated by the quantitative yeast two-hybrid analysis (Figs. 1 and 3). It is possible that this interaction alleviates the inhibitory effects posed by the SH3-SH2 domain on c-Abl kinase and therefore promotes c-Abl partial activation by releasing the SH2-kinase linker and enhancing Tyr^{245} autophosphorylation [27,31]. It is important to note that the full activation of c-Abl requires both Tyr^{245} autophosphorylation and additional stimuli such as IR-induced DNA damage. The functional significance of $hMSH5^{P29S}$ lies in the observation that this hMSH5 variant is less likely to be phosphorylated by c-Abl in response to IR-induced DNA damage, and as such sustains its interaction with c-Abl following IR exposure. Furthermore, these effects are directly associated with increased p73 accumulation and subsequent apoptosis in response to IR (Figs. 4B and 5A).

As a structural and functional p53 homolog, p73 can facilitate p53-independent DNA damage response [32], and it is known that the p53 network is often inactivated in human tumors through a number of different mechanisms [33]. Thus, it is particularly pertinent to understand p73-associated DNA damage responses in tumor cells harboring inactivated p53 protein or mutations of the p53 gene. In fact, 293T cells express an inactive p53 polypeptide resulting from the binding of the SV40 large T antigen, thus providing a p53-negative experimental system for addressing the effects of hMSH5/c-Abl specifically on the activation of p73 and related apoptosis in response to DNA damage.

It is worthy of note that IR exposure triggers a rapid induction of the endogenous hMSH5 protein. Clearly, blocking of IR-triggered hMSH5 induction by RNAi reduces p73 accumulation and the corresponding apoptotic response. Together, the current evidence suggest that the expression of hMSH5 is normally maintained at a low level in unperturbed cells, therefore DNA damage triggered hMSH5 induction could represent one of the important factors for regulation of DNA damage response—most likely by a scenario that a big increase in the level of hMSH5 would promote apoptotic response, whereas a moderate induction could facilitate DNA DSB repair.

Given the observation that the expression of Msh5 increases during the initiation of meiotic HR in male mice and the c-Abl-p73 pathway can be activated in response to IR in p53 negative male germ cells [34,35], our current finding has also raised the possibility that the hMSH5-c-Abl-p73 pathway might play a role in spontaneous germ cell apoptosis. In particular, the effect of $hMSH5^{P29S}$ on promoting mitotic apoptosis can be expected to have a mirrored impact on germ cell apoptosis. In this regard, it is interesting to note that the *hMSH5*^{P29S} allele frequency is positively correlated with the extent of germ cell apoptosis in Chinese and non-Hispanic Caucasian men [25,36,37], thus implicating a potential link between hMSH5, c-Abl-p73 activation, and germ cell apoptosis.

The activation of c-Abl-p73 in DNA damage response by members of the MMR family of proteins is not unprecedented. For instance, hMLH1 has been shown to play a critical role in mediating the activation of c-Abl-p73-dependent apoptosis in response to cisplatin treatment [19]. However, hMLH1 is not involved in mediating DNA damage response triggered by IR exposure [38,39], suggesting that the c-Abl-p73-dependent apoptotic response could be dynamically regulated and selectively activated by certain types of genotoxic insults through differential activation of DNA damage sensing proteins. This idea is supported by the observation that ultraviolet (UV) radiation can induce dose-dependent hMSH5 degradation (data not shown). Incidentally, UV irradiation does not induce c-Abl activation [40,41], suggesting that the hMSH5-cAbl-p73-initiated caspase-dependent apoptosis might be specific to certain DNA damages including those induced by IR. However, the delineation of this issue awaits further exploration of the molecular mechanisms involved with hMSH5 in DNA damage response and repair.

In addition to the immediate effect on dissociating the hMSH5-c-Abl complex, the direct role(s) of hMSH5 tyrosine phosphorylation in DNA damage response and/or DNA repair remains to be addressed. It is known that hRad51 co-exists with hMSH5 and c-Abl in the same protein complex [36], and phosphorylation of hRad51 by c-Abl or Bcr-Abl can enhance recombinational repair of DSBs and therefore increase genotoxic drug resistance [13,14]. It is very likely that phosphorylation could regulate the action of hMSH5 in DNA recombinational repair. In fact, recent work in our laboratory has indicated that disruption of c-Abl mediated hMSH5 phosphorylation impairs HR repair of DNA DSBs (Tompkins et al., manuscript in preparation). Lastly, it is currently unclear whether tyrosine phosphorylation plays any role in the nuclear/cytoplasmic distribution of hMSH5, as a recent study has clearly demonstrated that the sub-cellular localization of hMSH5 is subjected to dynamic regulation in cells [42].

In summary, our current study implies that altering the interaction between hMSH5 and c-Abl can mediate abnormal cellular responses to radiotherapy and radiomimetic anti-cancer drugs. The strong anti-apoptotic effect of c-Abl inhibition on IR-induced cell killing suggests that caution should be taken when c-Abl kinase inhibitors are combined with radiotherapy in anti-cancer regimens, especially for p53 negative tumors. Clearly, a thorough study of the molecular mechanisms involved with hMSH5 and c-Abl in the processes of DNA damage response and recombinational repair is required for a better understanding of their impacts not only on cancer development but also on cellular responses to antineoplastic drug treatments.

Acknowledgments

We thank Dr. Wei Yi, Dr. Nianxi Zhao, and Tai-Hsien Lee for their technical assistance in generating and analyzing 293T/hMSH5^{P29S} stable cell line, and Anoria K. Haick for proofreading the manuscript. Imatinib was kindly provided by Novartis Pharma AG, Basel, Switzerland. This work was supported in part by NIH Grant CA101796 (C.H.).

References

1. Her C, Doggett NA. Cloning, structural characterization, and chromosomal localization of the human orthologue of Saccharomyces cerevisiae MSH5 gene. Genomics. 1998; 52:50–61. [PubMed: 9740671]
2. de Vries SS, Baart EB, Dekker M, Siezen A, de Rooij DG, de Boer P, te Riele H. Mouse MutS-like protein Msh5 is required for proper chromosome synapsis in male and female meiosis. Genes Dev. 1999; 13:523–531. [PubMed: 10072381]

3. Edelmann W, Cohen PE, Kneitz B, Winand N, Lia M, Heyer J, Kolodner R, Pollard JW, Kucherlapati R. Mammalian MutS homologue 5 is required for chromosome pairing in meiosis. Nat Genet. 1999; 21:123–127. [PubMed: 9916805]
4. Sekine H, Ferreira RC, Pan-Hammarström Q, Graham RR, Ziemba B, de Vries SS, Liu J, Hippen K, Koeuth T, Ortmann W, Iwahori A, Elliott MK, Offer S, Skon C, Du L, Novitzke J, Lee AT, Zhao N, Tompkins JD, Altshuler D, Gregersen PK, Cunningham-Rundles C, Harris RS, Her C, Nelson DL, Hammarström L, Gilkeson GS, Behrens TW. Role for Msh5 in the regulation of Ig class switch recombination. Proc Natl Acad Sci USA. 2007; 104:7193–7198. [PubMed: 17409188]
5. Kato T, Sato N, Hayama S, Yamabuki T, Ito T, Miyamoto M, Kondo S, Nakamura Y, Daigo Y. Activation of Holliday Junction recognizing protein involved in the chromosomal stability and immortality of cancer cells. Cancer Res. 2007; 67:8544–8553. [PubMed: 17823411]
6. Snowden T, Acharya S, Butz C, Berardini M, Fishel R. hMSH4-hMSH5 recognizes Holliday Junctions and forms a meiosis-specific sliding clamp that embraces homologous chromosomes. Mol Cell. 2004; 15:437–451. [PubMed: 15304223]
7. Guikema JE, Schrader CE, Leus NG, Ucher A, Linehan EK, Werling U, Edelmann W, Stavnezer J. Reassessment of the role of Mut S homolog 5 in Ig class switch recombination shows lack of involvement in cis- and trans-switching. J Immunol. 2008; 181:8450–8459. [PubMed: 19050263]
8. Wang Y, Broderick P, Webb E, Wu X, Vijayakrishnan J, Matakidou A, Qureshi M, Dong Q, Gu X, Chen WV, Spitz MR, Eisen T, Amos CI, Houlston RS. Common 5p15.33 and 6p21.33 variants influence lung cancer risk. Nat Genet. 2008; 40:1407–1409. [PubMed: 18978787]
9. Yi W, Lee TH, Tompkins JD, Zhu F, Wu X, Her C. Physical and functional interaction between hMSH5 and c-Abl. Cancer Res. 2006; 66:151–158. [PubMed: 16397227]
10. Baskaran R, Wood LD, Whitaker LL, Canman CE, Morgan SE, Xu Y, Barlow C, Baltimore D, Wynshaw-Boris A, Kastan MB, Wang JY. Ataxia telangiectasia mutant protein activates c-Abl tyrosine kinase in response to ionizing radiation. Nature. 1997; 387:516–519. [PubMed: 9168116]
11. Shafman T, Khanna KK, Kedar P, Spring K, Kozlov S, Yen T, Hobson K, Gatei M, Zhang N, Watters D, Egerton M, Shiloh Y, Kharbanda S, Kufe D, Lavin MF. Interaction between ATM protein and c-Abl in response to DNA damage. Nature. 1997; 387:520–523. [PubMed: 9168117]
12. Kharbanda S, Yuan ZM, Wichselbau R, Kufe D. Determination of cell fate by c-Abl activation in response to DNA damage. Oncogene. 1998; 17:3309–3318. [PubMed: 9916993]
13. Chen G, Yuan SS, Liu W, Xu Y, Trujillo K, Song B, Cong F, Goff SP, Wu Y, Arlinghaus R, Baltimore D, Gasser PJ, Park MS, Sung P, Lee EY. Radiation-induced assembly of Rad51 and Rad52 recombination complex requires ATM and c-Abl. J Biol Chem. 1999; 274:12748–12752. [PubMed: 10212258]
14. Slupianek A, Schmutte C, Tombline G. BCR/ABL regulates mammalian RecA homologs, resulting in drug resistance. Mol Cell. 2001; 8:795–806. [PubMed: 11684015]
15. Déry U, Masson JY. Twists and turns in the function of DNA damage signaling and repair proteins by post-translational modifications. DNA Repair (Amst). 2007; 6:561–577. [PubMed: 17258515]
16. Pendergast AM. The Abl family kinases: mechanisms of regulation and signaling. Adv Cancer Res. 2002; 85:51–100. [PubMed: 12374288]
17. Wang JY. Controlling Abl: auto-inhibition and co-inhibition? Nat Cell Biol. 2004; 6:3–7. [PubMed: 14704671]
18. Agami R, Blandino G, Oren M, Shaul Y. Interaction of c-Abl and p73α and their collaboration to induce apoptosis. Nature. 1999; 399:809–813. [PubMed: 10391250]
19. Gong JG, Costanzo A, Yang HQ, Melino G, Kaelin WG Jr, Levrero M, Wang JY. The tyrosine kinase c-Abl regulates p73 in apoptotic response to cisplatin-induced DNA damage. Nature. 1999; 399:806–809. [PubMed: 10391249]
20. Yuan ZM, Shioya H, Ishiko T, Sun X, Gu J, Huang YY, Lu H, Kharbanda S, Weichselbaum R, Kufe D. p73 is regulated by tyrosine kinase c-Abl in the apoptotic response to DNA damage. Nature. 1999; 399:814–817. [PubMed: 10391251]
21. Scheijen B, Griffin JD. Tyrosine kinase oncogenes in normal hematopoiesis and hematological disease. Oncogene. 2002; 21:3314–3333. [PubMed: 12032772]
22. Lin J, Arlinghaus R. Activated c-Abl tyrosine kinase in malignant solid tumors. Oncogene. 2008; 27:4385–4391. [PubMed: 18391983]

23. Vo AT, Zhu F, Wu X, Yuan F, Gao Y, Gu L, Li GM, Lee TH, Her C. hMRE11 deficiency leads to microsatellite instability and defective DNA mismatch repair. EMBO Rep. 2005; 6:438–444. [PubMed: 15864295]
24. Her C, Wu X, Griswold MD, Zhou F. Human MutS homologue MSH4 physically interacts with von Hippel-Lindau tumor suppressor-binding protein 1. Cancer Res. 2003; 63:865–872. [PubMed: 12591739]
25. Yi W, Wu X, Lee TH, Doggett NA, Her C. Two variants of MutS homolog hMSH5: prevalence in humans and effects on protein interaction. Biochem Biophys Res Commun. 2005; 332:524–532. [PubMed: 15907804]
26. Mandon-Pépin B, Touraine P, Kuttenn F, Derbois C, Rouxel A, Matsuda F, Nicolas A, Cotinot C, Fellous M. Genetic investigation of four meiotic genes in women with premature ovarian failure. Eur J Endocrinol. 2008; 158:107–115. [PubMed: 18166824]
27. Brasher BB, Van Etten RA. c-Abl has high intrinsic tyrosine kinase activity that is stimulated by mutation of the Src homology 3 domain and by autophosphorylation at two distinct regulatory tyrosines. J Biol Chem. 2000; 275:35631–35637. [PubMed: 10964922]
28. Leong C, Vidnovic N, DeYoung MP, Sgroi D, Ellison LW. The p63/p73 network mediates chemosensitivity to cisplatin in a biologically defined subset of primary breast cancers. J Clin Invest. 2007; 117:1370–1380. [PubMed: 17446929]
29. Lin KW, Nam SY, Toh WH, Dulloo I, Sabapathy K. Multiple stress signals induce p73β accumulation. Neoplasia. 2004; 6:546–557. [PubMed: 15548364]
30. Bouquet F, Muller C, Salles B. The loss of gammaH2AX signal is a marker of DNA double strand breaks repair only at low levels of DNA damage. Cell Cycle. 2006; 5:1116–1122. [PubMed: 16721046]
31. Nagar B, Hantschel O, Seeliger M, Davies JM, Weis WI, Superti-Furga G, Kuriyan J. Organization of the SH3-SH2 unit in active and inactive forms of the c-Abl tyro-sine kinase. Mol Cell. 2006; 21:787–798. [PubMed: 16543148]
32. Yuan ZM, Huang Y, Ishiko T, Kharbanda S, Weichselbaum R, Kufe D. Regulation of DNA damage-induced apoptosis by c-Abl tyrosine kinase. Proc Natl Acad Sci USA. 1997; 94:1437–1440. [PubMed: 9037071]
33. Petitjean A, Acatz MIW, Borresen-Dale AL, Hainaut P, Olivier M. *TP53* mutations in human cancers: functional selection and impact on cancer prognosis and outcomes. Oncogene. 2007; 26:2157–2165. [PubMed: 17401424]
34. Lee TH, Yi W, Griswold MD, Zhu F, Her C. Formation of hMSH4-hMSH5 hetero-complex is a prerequisite for subsequent GPS2 recruitment. DNA Repair (Amst). 2006; 5:32–42. [PubMed: 16122992]
35. Hamer G, Gademan IS, Kal HB, de Rooij DG. Role for c-Abl and p73 in the radiation response of male germ cells. Oncogene. 2001; 20:4298–4304. [PubMed: 11466610]
36. Her C, Zhao N, Wu X, Tompkins JD. MutS homologues hMSH4 and hMSH5: diverse functional implications in humans. Front Biosci. 2007; 12:905–911. [PubMed: 17127347]
37. Hikim AP, Wang C, Lue Y, Johnson L, Wang XH, Swerdloff RS. Spontaneous germ cell apoptosis in humans: evidence for ethnic differences in the susceptibility of germ cells to programmed cell death. J Clin Endocrinol Metab. 1998; 83:152–156. [PubMed: 9435433]
38. Papouli E, Cejka P, Jiricny J. Dependence of the cytotoxicity of DNA-damaging agents on the mismatch repair status of human cells. Cancer Res. 2004; 64:3391–3394. [PubMed: 15150090]
39. Yan T, Schupp JE, Hwang HS, Wagner MW, Berry SE, Strickfaden S, Veigl ML, Sedwick WD, Boothman DA, Kinsella TJ. Loss of DNA mismatch repair imparts defective cdc2 signaling and G(2) arrest responses without altering survival after ionizing radiation. Cancer Res. 2001; 61:8290–8297. [PubMed: 11719462]
40. Liu ZG, Baskaran R, Lea-Chou ET, Wood LD, Chen Y, Karin M, Wang JY. Three distinct signaling responses by murine fibroblasts to genotoxic stress. Nature. 1996; 384:273–276. [PubMed: 8918879]
41. Cong F, Tang J, Hwang BJ, Vuong BQ, Chu G, Goff SP. Interaction between UV-damaged DNA binding activity proteins and the c-Abl tyrosine kinase. J Biol Chem. 2002; 277:34870–34878. [PubMed: 12107171]

42. Neyton S, Lespinasse F, Lahaye F, Staccini P, Paquis-Flucklinger V, Santucci-Darmanin S. CRM1-dependent nuclear export and dimerization with hMSH5 contribute to the regulation of hMSH4 subcellular localization. Exp Cell Res. 2007; 313:3680–3693. [PubMed: 17869244]

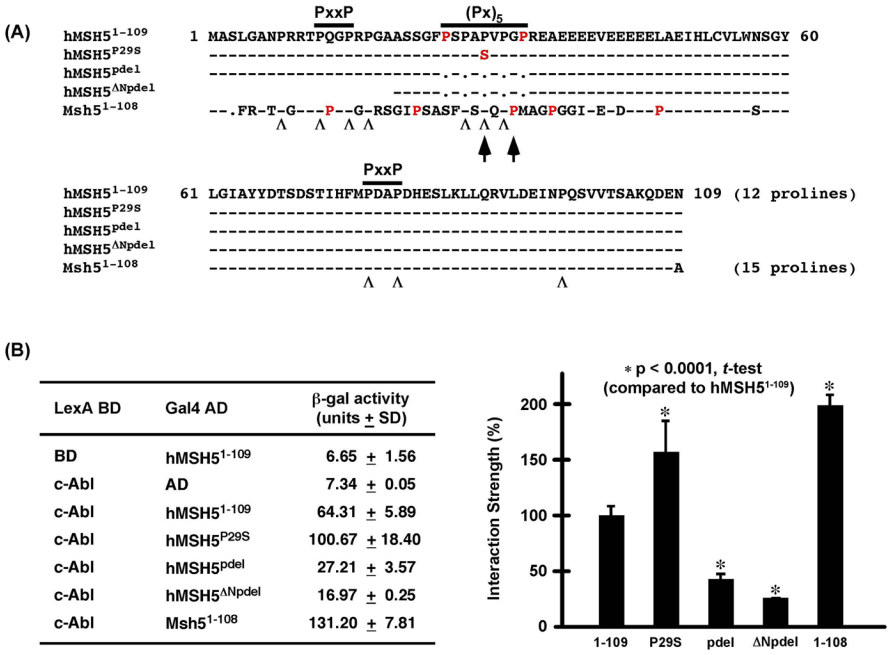

LexA BD	Gal4 AD	β-gal activity (units ± SD)
BD	hMSH5 1-109	6.65 ± 1.56
c-Abl	AD	7.34 ± 0.05
c-Abl	hMSH5 1-109	64.31 ± 5.89
c-Abl	hMSH5 P29S	100.67 ± 18.40
c-Abl	hMSH5 pdel	27.21 ± 3.57
c-Abl	hMSH5 ΔNpdel	16.97 ± 0.25
c-Abl	Msh5 1-108	131.20 ± 7.81

Figure 1.

Yeast two-hybrid analysis of the interaction between the proline-rich NH_2-terminal region and c-Abl SH3 domain. (**A**) Amino acid sequence alignment of the hMSH5 mutants and the comparable region of the mouse Msh5 used in the analysis. Besides the $(Px)_5$ and PxxP motifs, the third Msh5 PxxP motif is highlighted by two arrows, and "Λ" sings are used to designate conserved Pro residues between the human and mouse sequences while non-conserved Pro residues are in red. Black dots represent gaps or deletions and dashes represent identical residues in the sequences. (**B**) ONPG-based β-galactosidase liquid assay of L40 double transformants expressing different pairs of fusion proteins. Protein interaction strength is presented as an average β-gal activity unit of at least three independent measurements, and is also shown in the form of bar graphs for the comparison of relative protein interactions. Error bars are standard deviations from the mean, and statistical analysis was performed with Student's t-test.

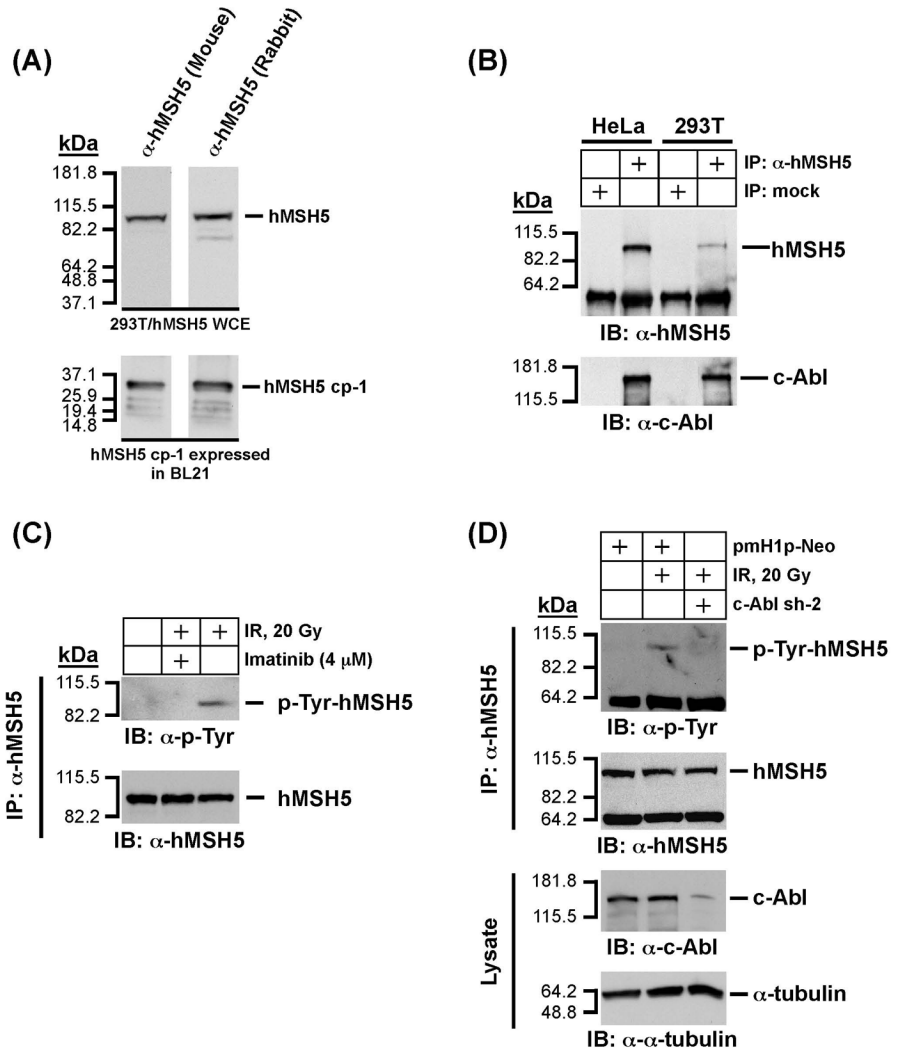

Figure 2.

Analysis of physical and functional interaction between endogenous hMSH5 and cAbl. (**A**) Characterization of a new mouse α-hMSH5 antiserum. Immunoblotting of 293T/hMSH5 whole cell extract (WCE) and partially purified bacterially expressed antigen hMSH5 cp-1 was performed with both the new mouse antiserum and the affinity-purified rabbit α-hMSH5 antibody. (**B**) Co-IP analysis of endogenous protein interaction between hMSH5 and c-Abl. Cell extracts prepared from approximately 0.1 ml of HeLa or 293T cell pellets were used to perform co-IP with 10 μl of the mouse α-hMSH5 antiserum. The presence of hMSH5 and cAbl in the immunoprecipitates was analyzed by Western blotting with α-hMSH5 and α-c-Abl antibodies. (**C**) The effect of c-Abl inhibition by imatinib on hMSH5 phosphorylation in response to IR in 293T cells. One hour after exposure to 20 Gy IR, cell extract was prepared and used to immunopurify hMSH5 with the mouse α-hMSH5 antibody. The status of hMSH5 tyro-sine phosphorylation was evaluated with an α-p-Tyr immunobot. To inhibit c-Abl activity, cells were pretreated with 4 uM imatinib 48 h prior to IR treatment. (**D**) Effect of c-Abl RNAi on IR-triggered hMSH5 phosphorylation. Cells were transfected with c-Abl sh-2 (or empty pmH1P-Neo vector as a control) at 48 h prior to IR treatment. The efficiency of c-Abl knockdown was validated with an α-c-Abl immunoblot, and its effect on IR-triggered hMSH5 phosphorylation was assessed by α-p-Tyr immunobotting. The α-tubulin blot was used as a loading control. *kDa*, molecular weight (*Mr*) in thousands.

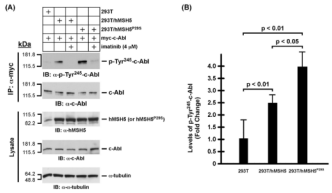

Figure 3.

Analysis of c-Abl autophosphorylation in 293T, 293T/hMSH5, and 293T/hMSH5^{P29S} cells. (**A**) Examination of autophosphorylation of c-Abl at Tyr^{245}. To compensate for the elevated levels of hMSH5, c-Abl was overexpressed by transfection of cells with a myc-c-Abl encoding construct. Assessment of c-Abl autophosphorylation was performed with α-phospho-cAbl (Tyr^{245}) immunoblotting of α-myc immunoprecipitates, while α-c-Abl immunoblot was used as a loading control. Equivalent and stable expressions of hMSH5 or hMSH5^{P29S} in reference to the endogenous hMSH5 are also shown in the lower "Lysate" panel. (**B**) The average levels and standard deviations (error bars) of c-Abl Tyr^{245} autophosphorylation were determined from three measurements, and the p-values of the *t*-tests are indicated.

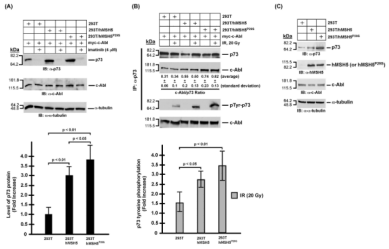

Figure 4.

Analysis of p73 protein accumulation and phosphorylation in 293T, 293T/hMSH5, and 293T/hMSH5^{P29S} cells. It is known that both p73αand p73β are stabilized by c-Abl and both undergo c-Abl dependent tyrosine phosphorylation in response to IR, of which p73β was particularly examined in these experiments [20,28,29]. (**A**) Immunoblotting analysis of p73 accumulation in 293T, 293T/hMSH5, and 293T/hMSH5^{P29S} cells. Blots of α-tubulin and c-Abl were used as loading controls. Levels of p73 protein was determined from at least three experiments and quantified for the relative increases of p73 accumulation above that of the untreated 293T cells. Error bars are standard deviation from the mean (bar graph, lower panel). (**B**) Analysis of the interaction between p73 and c-Abl, as well as p73 tyrosine phosphorylation 1 h after IR exposure. 293T, 293T/hMSH5, and 293T/hMSH5^{P29S} cells were transfected to express myc-c-Abl prior to exposure to 20 Gy IR. Co-IP was performed with α-p73 and the resulting immunoprecipitates were used to analyze the amounts of p73 and c-Abl proteins as well as the status of p73 tyrosine phosphorylation. The average c-Abl/p73 ratios (representing the relative levels of these two proteins in the immunoprecipitates) and standard deviations were determined by three immunoblotting analyses of immunoprecipitates. The status of IR-triggered p73 tyrosine phospho-rylation was determined by the use of the α-p-Tyr antibody. The average levels of p73 phospho-rylation and corresponding standard deviations (error bars) were determined in three measurements (bar graph, lower panel). The levels of c-Abl in cell extracts are also shown. (**C**) Immunoblotting analysis of untransfected and untreated 293T, 293T/hMSH5, and 293T/hMSH5^{P29S} cells. *kDa*, molecular weight (*Mr*) in thousands.

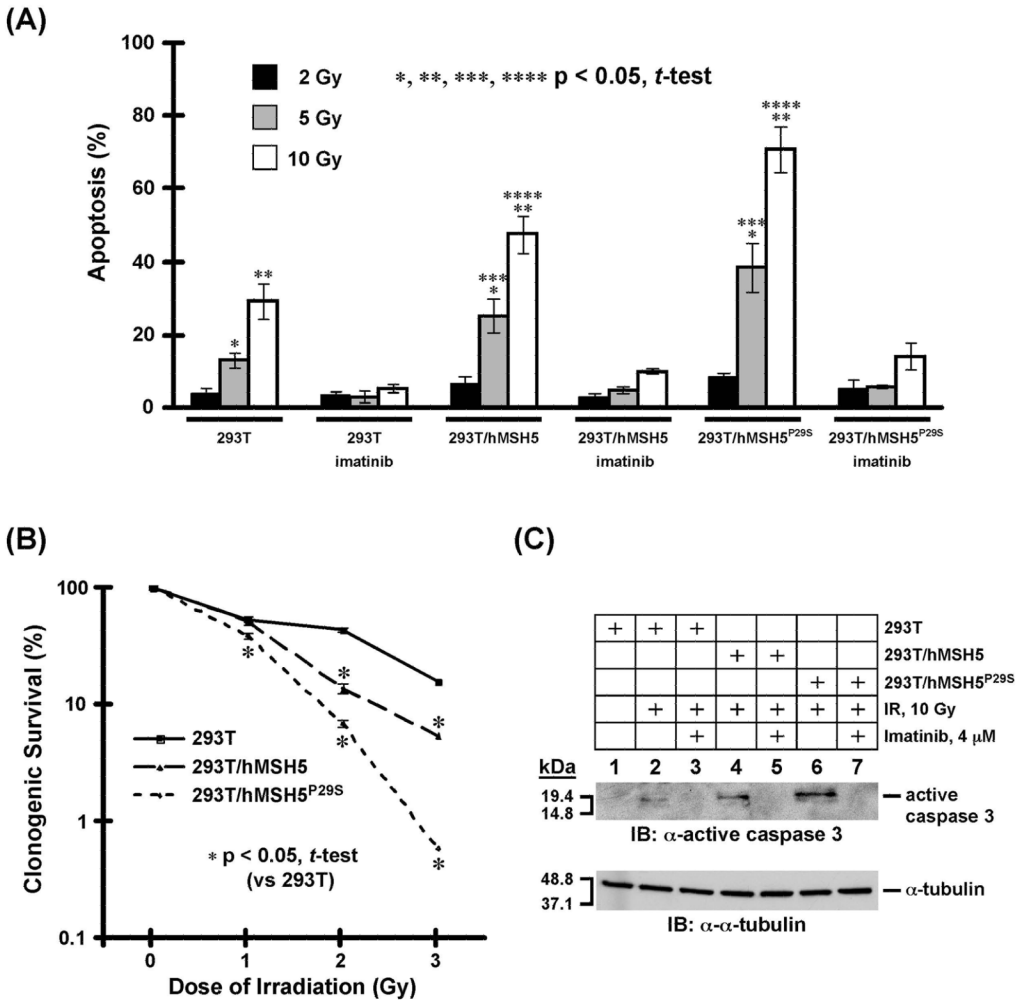

Figure 5.

Analysis of apoptotic response and survival of 293T, 293T/hMSH5, and 293T/hMSH5^{P29S} cells following IR exposure. (**A**) TUNEL analysis of IR triggered apoptotic responses. Cells were irradiated with 2, 5, and 10 Gy IR, and the levels of apoptosis were analyzed 24 h later. Without IR treatment and under identical experimental conditions, approximately 1% of cells were detected to be apoptotic for all three types of cells. Imatinib was used to inactivate c-Abl. The mean percentages and standard deviations (error bars) were determined from three independent data points. Statistically significant differences between cell lines are denoted with an asterisk. (**B**) Clonogenic survival analysis of 293T, 293T/hMSH5 and 293T/hMSH5^{P29S} cells treated with IR. Colonies that contained at least 50 cells were counted and the percentage of cell survival was determined in reference to untreated control cells. The means of three individual experiments and standard deviations (error bars) are presented, and asterisks are used to indicate significant differences between data points. (**C**) Analysis of cas-pase-3 activation in 293T, 293T/hMSH5, and 293T/hMSH5^{P29S} cells. Cells were treated with 10 Gy IR and analyzed after an additional 24 h in culture. Immunoblotting was conducted by the use of an α-active caspase-3 antibody. Imatinib was used to inhibit c-Abl, and α-tubulin blot was utilized as a loading control. *kDa*, molecular weight (*Mr*) in thousands.

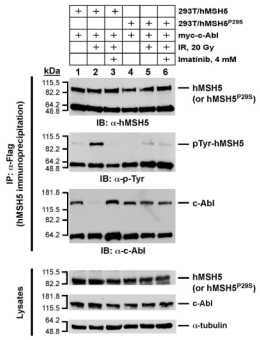

Figure 6.

The effects of P29S alteration on hMSH5-c-Abl interaction and tyrosine phosphorylation in response to IR-triggered DNA damage. 293T/hMSH5 and 293T/hMSH5^{P29S} cells were transfected with c-Abl and irradiated with 20 Gy IR. Cell extracts were prepared 1 h after IR treatment, and were used to perform hMSH5 immunoprecipitation by the use of α-Flag antibody. The resulting immunoprecipitates were analyzed by immunoblotting performed with α-hMSH5, α-p-Tyr, and α-c-Abl antibodies. Cell lysates were also analyzed to validate the expression of hMSH5 (or hMSH5^{P29S}) and c-Abl proteins in reference to the α-tubulin loading control. Imatinib pretreatment was utilized to inhibit c-Abl. *kDa*, molecular weight (*Mr*) in thousands.

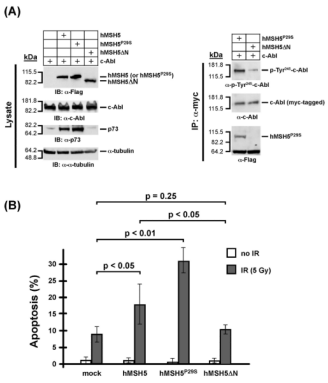

Figure 7.

The hMSH5-c-Abl interaction is important for stimulating c-Abl Tyr^{245} autophosphorylation and IR-triggered apoptosis (**A**) Immunoblotting of the expression of various forms of hMSH5 proteins and their effects on p73 accumulation. 293T cells were transfected with c-Abl, or together with hMSH5, $hMSH5^{P29S}$, or hMSH5ΔN. Cell extracts were prepared 48 h post-transfection, and levels of protein expression were analyzed by immunoblotting (left panel). The α-myc immunoprecipitates were used to analyze c-Abl autophosphorylation at Tyr^{245} and its interaction with $hMSH5^{P29S}$ or hMSH5ΔN (right panel). (**B**) TUNEL analysis of the effect of hMSH5ΔN on IR-triggered apoptosis. 293T cells were transiently transfected to express hMSH5, $hMSH5^{P29S}$, or hMSH5ΔN 48 h prior to 5 Gy IR exposures, in which mock-transfected cells were used as controls. The rates of apoptosis were determined 24 h post-IR treatment. Mean percentages and standard deviations (error bars) were shown on the basis of three independent data points. *P*-values are indicated for statistical analysis.

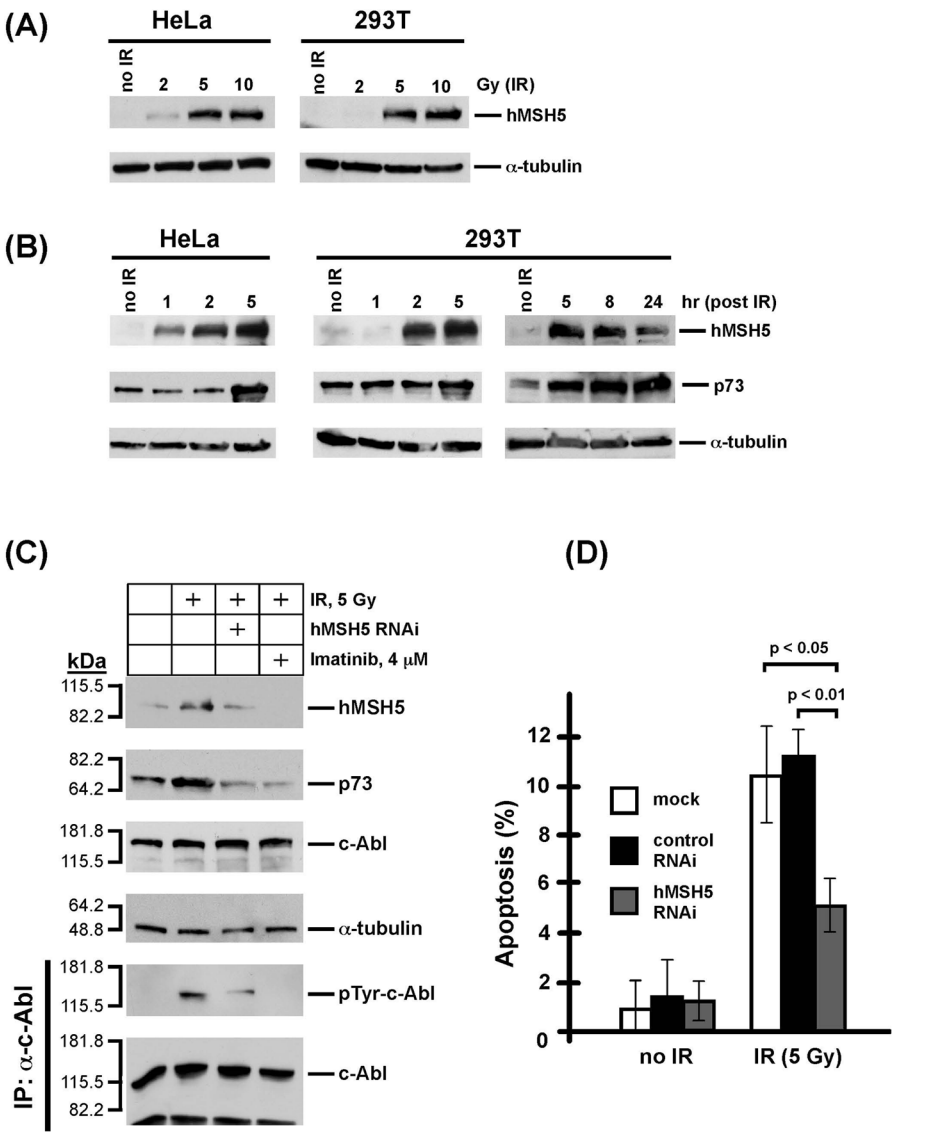

Figure 8.

IR-triggered endogenous hMSH5 accumulation and apoptosis. (**A**) IR dose-dependent hMSH5 induction in HeLa and 293T cells. The levels of hMSH5 induction were evaluated 2 h after each treatment in reference to the level of α-tubulin. (**B**) Analysis of hMSH5 induction and p73 accumulation at various times after IR exposure. HeLa and 293T cells were irradiated with 5 Gy IR and cell lysates were prepared at various times as indicated. Immunoblot of α-tubulin was used as a loading control. (**C**) Effects of hMSH5 RNAi and imatinib on IR-triggered hMSH5 induction and p73 accumulation. 293T cells were transfected with hMSH5 sh-2 and treated with 5 Gy IR at 48 h post transfection, and the levels of proteins were evaluated 5 h after irradiation. Imatinib was used to inhibit c-Abl kinase activity. *kDa*, molecular weight (*Mr*) in thousands. (**D**) Preventing IR-triggered hMSH5 induction by RNAi compromised apoptosis. 293T cells were transfected with hMSH5 sh-2 or a control RNAi construct (pmH1P-Neo/NT, see Materials and Methods), of which the latter had no effect on hMSH5 expression (data not shown). Cells were exposed to 5 Gy IR at 48 h after transfection. Apoptosis was analyzed by TUNEL 24 h following

irradiation. Error bars represent standard deviation from the mean of three data points. *P*-values are provided for significant differences.